THE JOURNAL OF PHYSICAL CHEMISTRY B

Article

pubs.acs.org/JPCB

Accurate Description of Aqueous Carbonate Ions: An Effective Polarization Model Verified by Neutron Scattering

Philip E. Mason,* Erik Wernersson, and Pavel Jungwirth*

Institute of Organic Chemistry and Biochemistry, Academy of Sciences of the Czech Republic, Flemingovo nám. 2, 16610 Prague 6, Czech Republic

Supporting Information

ABSTRACT: The carbonate ion plays a central role in the biochemical formation of the shells of aquatic life, which is an important path for carbon dioxide sequestration. Given the vital role of carbonate in this and other contexts, it is imperative to develop accurate models for such a high charge density ion. As a divalent ion, carbonate has a strong polarizing effect on surrounding water molecules. This raises the question whether it is possible to describe accurately such systems without including polarization. It has recently been suggested the lack of electronic polarization in nonpolarizable water models can be effectively compensated by introducing an electronic dielectric continuum, which is with respect to the forces between atoms equivalent to rescaling the ionic charges. Given how widely nonpolarizable models are used to model electrolyte solutions, establishing the experimental validity of this suggestion is imperative. Here, we examine a stringent test for such models: a comparison of the difference of the neutron scattering structure factors of K_2CO_3 vs KNO_3 solutions and that predicted by molecular dynamics simulations for various models of the same systems. We compare standard nonpolarizable simulations in SPC/E water to analogous simulations with effective ion charges, as well as simulations in explicitly polarizable POL3 water (which, however, has only about half the experimental polarizability). It is found that the simulation with rescaled charges is in a very good agreement with the experimental data, which is significantly better than for the nonpolarizable simulation and even better than for the explicitly polarizable POL3 model.

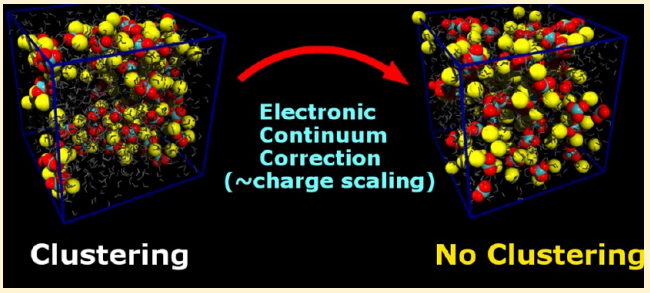

INTRODUCTION

The importance of carbon dioxide in the atmosphere can hardly be overstated. The oceans currently act as a CO_2 sink that absorbs about a quarter of the anthropogenic CO_2 released into the atmosphere.[1] Of that, about 95% reacts with water to form monovalent hydrogen carbonate, and about 5% becomes the divalent carbonate ion. It is estimated that, by the end of the century, the CO_2 absorbed by the worlds oceans will have doubled the H^+ concentration of the oceans, leading to a decrease in pH from 8.1 to 7.8.[2] This will have the effect of lowering the levels of biologically available CO_3^{2-} used by marine organisms to make their $CaCO_3$ shells.[3] Given the importance of this CO_2 sink, it is therefore of vital importance that accurate molecular models of aqueous carbonate ions exist.

With the advent of fast and cheap computers, the molecular dynamics (MD) codes and models implemented on them have proven a potent tool over the past few decades. It is in many ways surprising, given the inherent quantum nature of the electronic structure and vibrational motions of water molecules, that water can be fairly successfully modeled within classical statistical mechanics with three simple point charges and a single van der Waals site.[3] Decades of use and refinement of water models demonstrate their scope and potential.[4] However, recent studies suggest a fundamental oversight in the parametrization of nonpolarizable models of ionic aqueous solutes.[5−8] Briefly, it is argued that, in water, the omission of explicit polarizability is reflected in the effective charges of empirical water models in a way that mimics an electronic dielectric continuum.[6,7] That the partial charges of empirical water models are *effective charges* is a fact that has been recognized since the advent of water models[9] and continues to be significant.[10] To make the treatment of electrostatic interactions consistent between the solute and the solvent, effective charges that take polarization effects into account should be used for both. Indeed, charge scaling is not uncommon in force field development,[11,12] and the values of the empirical screening factors may reflect dielectric-like screening as well as direct polarization or even charge transfer. However, for example, the charged groups in the CHARMM force field were not scaled in order to reproduce hydration free energies. This inconsistency has been resolved by adding the missing electronic terms into the free energy calculation.[7] If unscaled charges are used, the nonpolarizable simulation may not accurately reproduce the correct balance of ion−ion, ion−water, and water−water interactions in aqueous solutions.[6,7] This effect will

Received: January 25, 2012
Revised: May 14, 2012
Published: May 25, 2012

   dx.doi.org/10.1021/jp3008267 | J. Phys. Chem. B 2012, 116, 8145−8153

manifest itself already for monovalent ions but will be particularly significant for multivalent ions, which are capable of more strongly polarizing surrounding water molecules.[13]

The relationship between effective and actual charges is not obvious in general, but if the electronic polarization response is continuum-like, it follows that the ionic charges should simply be scaled by $1/\sqrt{\varepsilon_e}$, where ε_e is the part of the dielectric constant due to electronic degrees of freedom ($\varepsilon_e = 1.78$ for water).[8] Note that this gives the same result with respect to the forces between atoms as introducing an electronic dielectric continuum explicitly.[5] This results in what we refer to throughout this article as the Electronic Continuum Correction (ECC) model. Given the hundreds of studies performed involving aqueous electrolytes, the potential implications of this correction are vast, impacting on the accuracy of nonpolarizable simulation involving ions including parametrization of simple ions,[14] ion−ion[15,16] and ion−membrane association,[13] stabilization of peptide,[17,18] binding to proteins and amino acids,[19−21] etc. To examine experimentally the validity of the ECC model for a particularly challenging case of the divalent carbonate ion is the prime purpose of this article. Namely, we investigate how ion pairing and solution structure in K_2CO_3 and KNO_3 solutions vary between nonpolarizable, explicitly polarizable, and ECC models and then test these predictions via comparison to structural measurements made by neutron scattering experiments.

NEUTRON SCATTERING METHODS

The contrast between two solutions of near-identical atomic composition, 3 *m* K_2CO_3 and 3 *m* KNO_3, was examined by neutron scattering. Such high concentrations are necessary in order to achieve a suitable signal-to-noise ratio in the experimental measurement. In both solutions, the hydrogen composition was altered to make the average coherent neutron scattering length of the hydrogen nuclei zero (64.08% ^{1}H and 35.92% ^{2}H with coherent neutron scattering lengths of −3.741 fm and 6.674 fm for ^{1}H and ^{2}H, respectively), rendering them effectively neutron invisible. Neutron scattering patterns were obtained from the D20 diffractometer[22] at the Institut Laue Langevin, Grenoble, for solutions of 3.0 *m* K_2CO_3 and 3.0 *m* KNO_3 at a wavelength of 0.94 Å. These solutions were chosen due to their near-identical atomic compositions and for the fact that the NO_3^- and CO_3^{2-} ions are nearly structurally identical. These solutions were prepared by direct dissolution of the salts (dried in a vacuum oven for 4 h) in water. The total raw scattering patterns (collection time ≈ 1 h per sample) were measured at 23 °C, corrected for multiple scattering, incoherent scattering, and absorption, and normalized versus a standard vanadium rod to give the $F(Q)$s of the each respective solution using literature procedures.[23] $F(Q)$ can be written as

$$F(Q) = \sum_{\alpha}\sum_{\beta} c_\alpha c_\beta b_\alpha b_\beta (S_{\alpha\beta}(Q) - 1) \quad (1)$$

where $c_{\alpha \text{ or } \beta}$ is the atomic concentration of species α or β whose coherent neutron scattering length is $b_{\alpha \text{ or } \beta}$, and the summations are over all atomic species in the solution. $S_{\alpha\beta}(Q)$ is the partial structure factor of atoms α and β and is directly related to the radial pair distribution function $g_{\alpha\beta}(r)$ through Fourier transformation

$$g_{\alpha\beta}(r) - 1 = \frac{1}{2\pi^2\rho r}\int_0^\infty (S_{\alpha\beta}(Q) - 1)Q\,\sin(Qr)\mathrm{d}Q \quad (2)$$

While neutron scattering cannot distinguish chemically different nuclei of the same element, it is useful, as shall be seen later, to formally distinguish between the oxygens on water (Ow) and those on the oxyanion (Oi). The experimental neutron scattering measurement contains data on the spatial correlation between all non-hydrogen nuclei (Ow, K, Oi, and C or N), to all other non-hydrogen nuclei. Specifically, for the K_2CO_3 solution (an analogous expression can be written for the KNO_3 solution)

$$\begin{aligned}{}^{CO_3}F(Q) = [&(AS_{OwOw}(Q) + BS_{OwOi}(Q) + CS_{OwK}(Q)\\ &+ DS_{OwC}(Q) + ES_{OiOi}(Q) + FS_{OiK}(Q) + GS_{OiC}(Q)\\ &+ HS_{KK}(Q) + IS_{KC}(Q) + JS_{CC}(Q))/(A + B + C + D\\ &+ E + F + G + H + I + J)] - 1 \end{aligned} \quad (3)$$

The prefactors A−J are given in Table 1. Fourier transformation of ${}^{CO_3}F(Q)$ gives the function ${}^{CO_3}G(r)$, which contains

Table 1. Prefactors (As Calculated from the Product $c_\alpha c_\beta b_\alpha b_\beta$ in Eq 1) of the Experimental Neutron Scattering Measurements in This Study Grouped into the Water−Water (Red), Ion−Water (Green), and Ion−Ion (Blue) Terms

Correlation	K_2CO_3 solution	Prefactor [barn]		KNO_3 solution	Prefactor [barn]
A	Ow Ow	0.03050		Ow Ow	0.03050
B	Ow Oi	0.00988		Ow Oi	0.00988
C	Ow K	0.00421		Ow K	0.00421
D	Ow C	0.00377		Ow N	0.00531
E	Oi Oi	0.00080		Oi Oi	0.00080
F	Oi K	0.00068		Oi K	0.00068
G	Oi C	0.00061		Oi N	0.00086
H	K K	0.00015		K K	0.00015
I	C K	0.00026		N K	0.00037
J	C C	0.00012		N N	0.00023
Sum		0.05098			0.05299

information on the pairwise correlations between all atoms other than hydrogen

$$\begin{aligned}{}^{CO_3}G(r) = &(Ag_{OwOw}(r) + Bg_{OwOi}(r) + Cg_{OwK}(r)\\ &+ Dg_{OwC}(r) + Eg_{OiOi}(r) + Fg_{OiK}(r) + Gg_{OiC}(r)\\ &+ Hg_{KK}(r) + Ig_{KC}(r) + Jg_{CC}(r))\\ &/(A + B + C + D + E + F + G + H + I + J) \end{aligned} \quad (4)$$

Finally, we construct the difference functions by subtracting the results obtained from the two solutions. For reasons that are discussed elsewhere,[24] the reciprocal difference function is composed of the direct difference between the two sets of data ($\Delta F(Q) = {}^{CO_3}F(Q) - {}^{NO_3}F(Q)$), while the real space function is weighted by the number densities ($\Delta G(r) = \rho_{CO_3}\cdot{}^{CO_3}G(r) - \rho_{NO_3}\cdot{}^{NO_3}G(r)$).

SIMULATION DETAILS

Three sets of molecular dynamics simulations with different force fields were performed for both KNO_3 and K_2CO_3 solutions. The first employed the SPC/E water model,[25] the second the POL3 water model,[26] and the final set employed the SPC/E water model and effective ion charges as suggested recently by using the value 1.78 for the electronic dielectric constant ε_e.[5] These simulation runs are hereafter referred to as the SPC/E, POL3, and ECC simulations, respectively. MD simulations were carried

dx.doi.org/10.1021/jp3008267 | J. Phys. Chem. B 2012, 116, 8145−8153

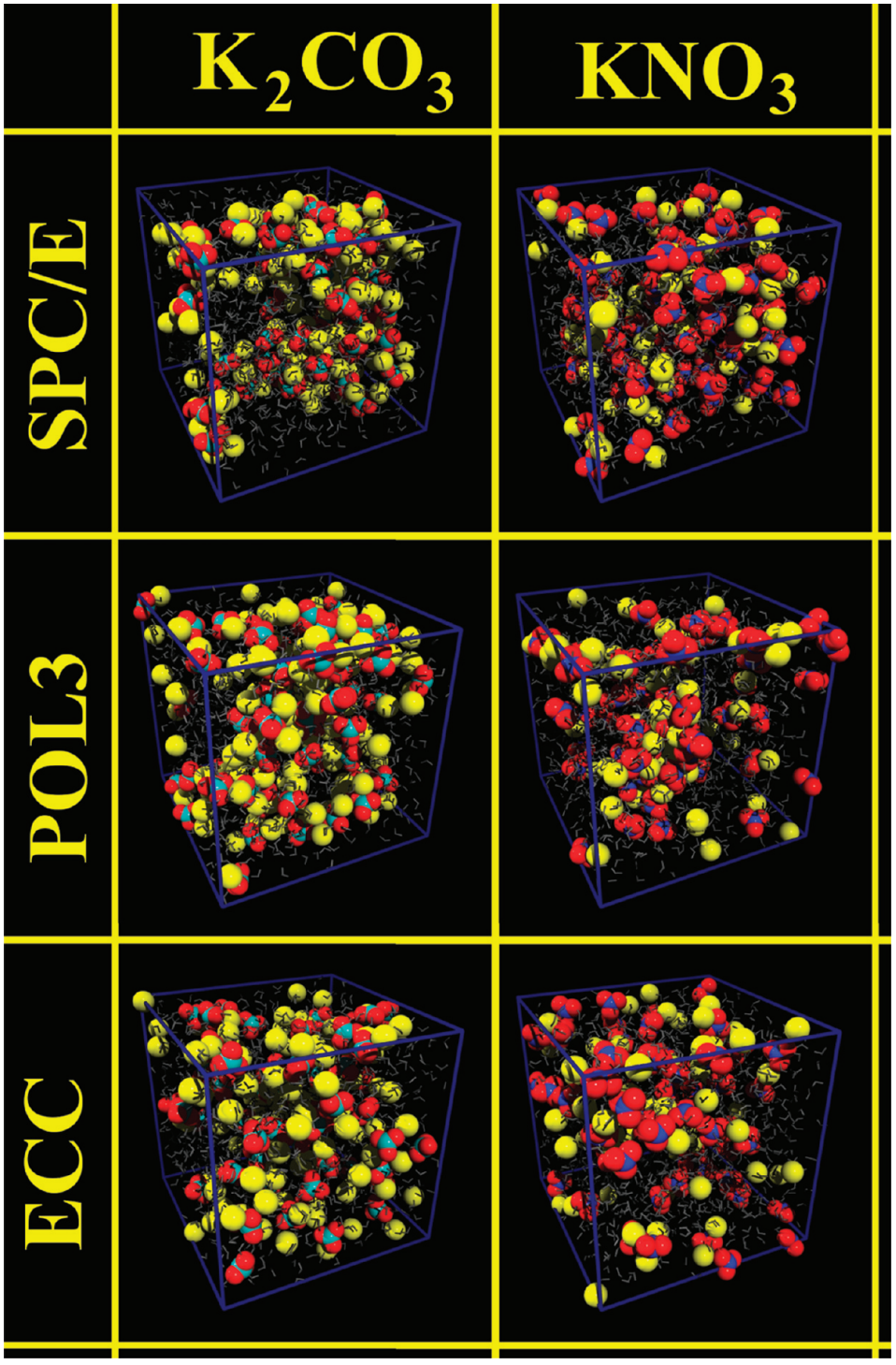

Figure 1. Representative snapshots of the three types of simulations presented in this study. Both the SPC/E and POL3 simulations show significantly more clustering for the K_2CO_3, than the ECC simulation. The effect of the different models on the KNO_3 simulations is less conspicuous. All MD graphics in this work were produced using VMD.[45]

out using the AMBER10 molecular dynamics program.[27] The K_2CO_3 simulations contained 132 potassium ions, 66 carbonate ions, and 1221 water molecules, while the KNO_3 simulations contained 66 potassium ions, 66 nitrate ions, and 1221 water molecules

For the potassium ions, we used the parameters of Dang et al.[28] For the oxyanions, the Lennard-Jones parameters and partial charges (for the central atom and oxygens, the charges were 0.8227 and −0.9409 e_0 for the carbonate and 0.6020 and −0.5340 e_0 for the nitrate) were taken from a previous study of Cs_2CO_3 and $CsNO_3$,[29] as were the bond parameters for the nitrogen−oxygen bond (an equilibrium distance of 1.21 Å). In the previous study, the NO bond and the CO bond were taken to have identical equilibrium distances.[29] For the nitrate, this was consistent with crystal structures, but for the carbonate, it was not.[30] Consequently, the equilibrium CO bond length in the present simulations was increased from 1.21 to 1.30 Å. For simulations with SPC/E, the ions were nonpolarizable. For the

dx.doi.org/10.1021/jp3008267 | J. Phys. Chem. B 2012, 116, 8145−8153

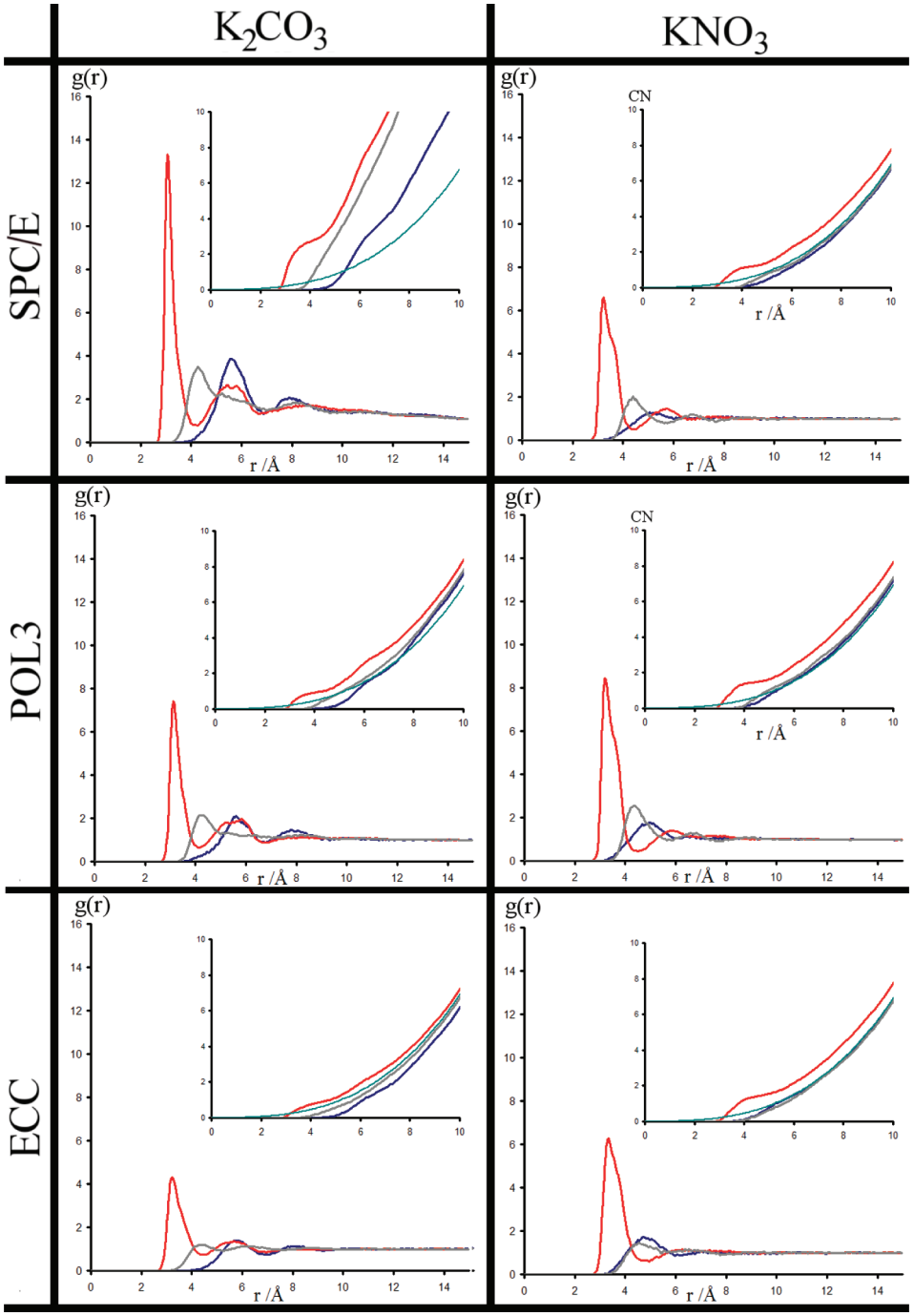

Figure 2. Ion−ion radial distribution functions. K−oxyanion $g(r)$ is shown in red, K−K $g(r)$ in gray, and oxyanion−oxyanion $g(r)$ in blue. In each case, the inset shows the rolling coordination numbers (same color coding with the green line being the rolling coordination number for a structureless point source matter ($g(r) = 1$)).

polarizible simulations, the polarizibility of potassium was 0.83 Å^3, and the nitrate and carbonate oxygens had polarizibilities of 1.0 and 0.6 Å^3, respectively. The practical reason for the lower value for carbonate is that higher values resulted in a polarization catastrophe.[31] Previous work on sulfate solutions indicates that water, rather than ion polarizability, is the decisive factor in determining the structure of solutions containing highly charged ions.[13] We, therefore, do not expect any severe artifacts due to the lower polarizability of the oxyanions. For the ECC simulations, the charges on the ions were scaled by $1/\sqrt{\varepsilon_e}$ (~0.75).[5]

After energy minimization and 500 ps of equilibration, the trajectories were propagated for 10 ns, using a time step of 1 fs. The temperature was kept at 300 K using a Berendsen thermostat.[32] To ensure that the experimental number densities were accurately reproduced, the box volumes were kept constant at the corresponding values, i.e., 41 265 Å^3 for K_2CO_3 and 41 179 Å^3 for KNO_3.

RESULTS AND DISCUSSION

Representative snapshots from the K_2CO_3 and KNO_3 solutions from the SPC/E, POL3, and ECC simulations are shown in

dx.doi.org/10.1021/jp3008267 | J. Phys. Chem. B 2012, 116, 8145−8153

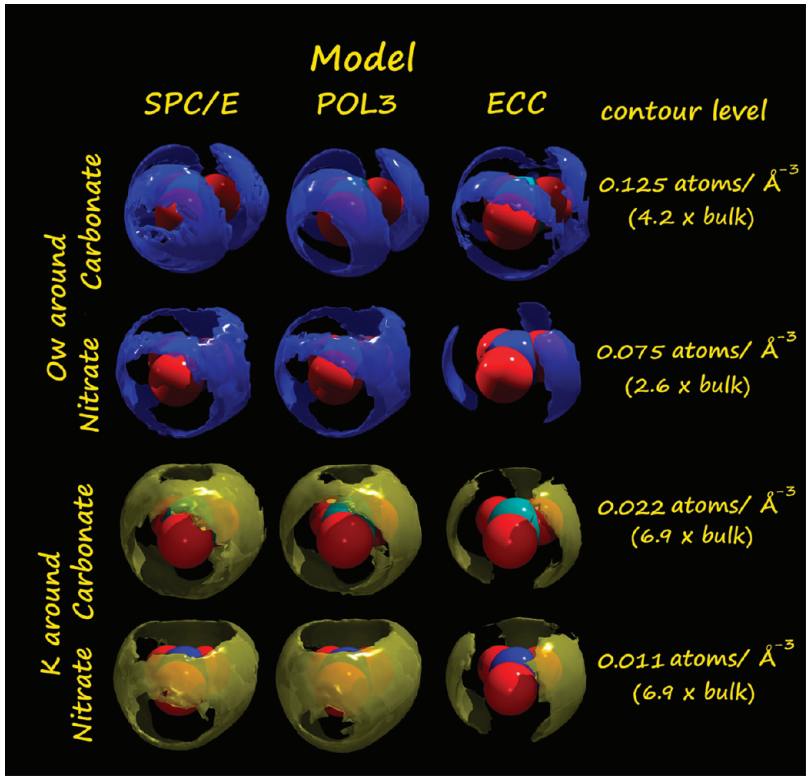

Figure 3. Density maps of water (blue) and potassium (yellow) around the oxyanion in the K_2CO_3 and KNO_3 simulations. The oxygen contour level was chosen to reflect best the form of the water−oxyanion structure and thus is at a higher level for the K_2CO_3 simulation than for the KNO_3 simulation, reflecting the stronger ordering around carbonate.

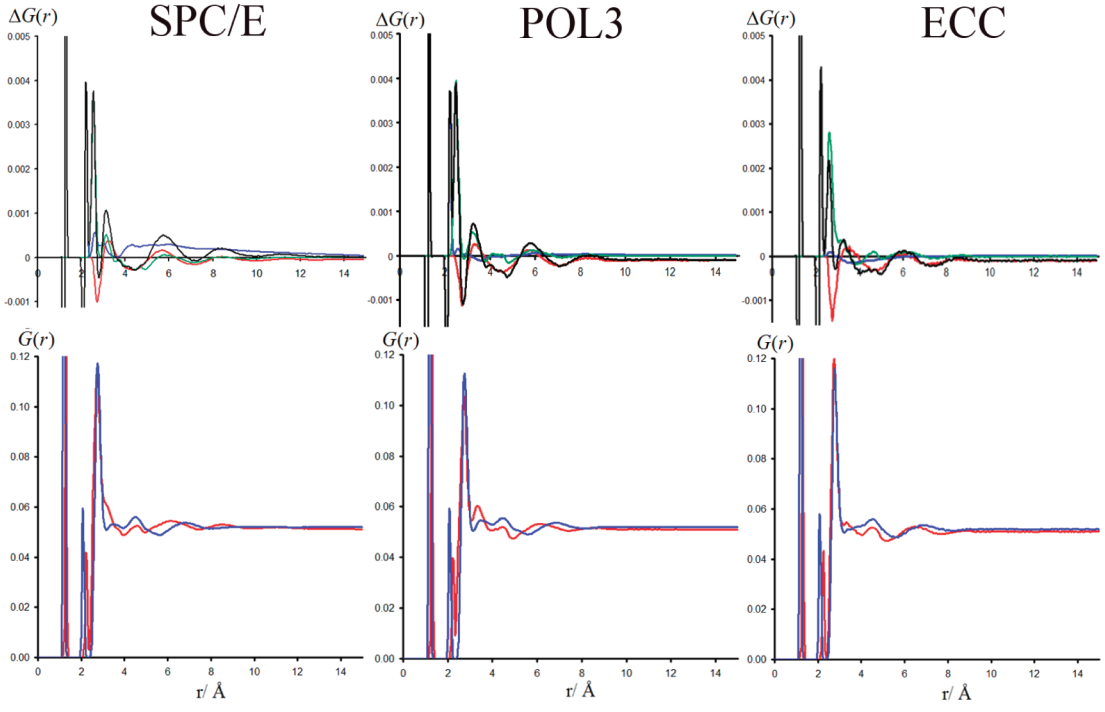

Figure 4. Functions $G(r)$ from the simulations for the K_2CO_3 and KNO_3 solutions (lower plots red and blue, respectively). The upper plots are the difference functions $\Delta G(r)$ for each pair of simulations (black). This is further divided into the components of this function due to water−water (red), water−ion (green), and ion−ion (blue) correlations.

Figure 1. The radial distribution functions $g(r)$ for each of the ion−ion correlations (in each case with respect to the center of mass of the ion) were calculated for each of the simulations along with the cumulative coordination numbers (i.e., the integrals of $g(r)$ from zero to a given distance, Figure 2). Both figures demonstrate the trend that the K_2CO_3 solution, for the SPC/E and POL3 simulations, exhibits strong ion-pairing and clustering resulting in extended ion structures, while the KNO_3 solution

dx.doi.org/10.1021/jp3008267 | J. Phys. Chem. B 2012, 116, 8145−8153

behaves in a more regular fashion, as expected from a monovalent electrolyte. The ion clustering can be seen in the snapshots but also in the ion−ion $g(r)$s remaining above unity out to about a nanometer for the SPC/E and POL3 simulations. No persistent extended structures were present in the ECC simulation, though there was some degree of transient clustering. The same effect is visible in the oxyanion−oxyanion cumulative coordination numbers when comparing the equivalent of a featureless distribution of oxyanions ($g(r) = 1$, green line in Figure 2), to the carbonate−carbonate cumulative coordination numbers, which are augmented (above ∼5 Å) for both SPC/E and POL3 but not for the ECC simulation. The degree of ion pairing and clustering is smaller in the POL3 simulation than in the SPC/E simulation but still higher than for the ECC run. Arguably one of the most direct demonstrations of this is the height of the oxyanion−potassium peak. It is possible to anticorrelate the degree of pairing in the high charge density case of the K_2CO_3 solution to the degree to which polarizibility is accounted for in the simulations. In the nonpolarizable SPC/E simulation, the peak height for oxyanion−potassium peak is ∼14, while the POL3 simulation with about half of polarization included (vide infra) has a peak height of ∼8, and finally the ECC simulation, which effectively emulates 100% of the polarizibility, has a peak height of ∼4. For the nitrate simulations with the lower charge density ion, this trend is less evident, and the variations between the three simulations are smaller. The density maps for water and potassium around the oxyanion were calculated for all simulations (Figure 3) and show a decrease in the solvent shell density and ordering for the ECC simulations compared to the SPC/E and POL3 simulations.

Before moving on to extract from the simulations the functions $G(r)$ and $\Delta G(r)$ and compare these results with the neutron scattering data, it is worth noting that, in principle, POL3 and ECC should, if polarization is treated sufficiently accurately, give similar results. However, the ion association in the POL3 K_2CO_3 solution is far stronger than in the ECC simulations. A similar, albeit more subtle trend is found in the KNO_3 simulations. We note that the overall dipole polarizability of POL3 water (0.868 $Å^3$) is significantly smaller than the gas phase experimental value (1.44 $Å^3$). It may thus be fairer to characterize the POL3 as merely a partly polarizable model. These observations put the POL3 model in a position between the nonpolarizible SPC/E model and the ECC model, with the latter accounting for full electronic polarizibility, albeit in an effective manner.

The function $G(r)$ (eq 4) and the difference function $\Delta G(r)$ were calculated for all the simulations (Figure 4). The sharp peaks at ∼1.2 and 2.1 Å are the intramolecular correlations of the oxyanion, occurring at slightly different positions due to the marginally different nitrate and carbonate geometries. The difference function $\Delta G(r)$ provides a clearer representation of the different hydration of these two ions as the functions $G(r)$ tend to be dominated by comparable water−water correlations, which are similar for both solutions. In the MD data, $\Delta G(r)$ can be broken down into the components due to the differences in the water−water, ion−water, and ion−ion structures between the CO_3^{2-} and NO_3^- solutions. From this, the difference in ion pairing and clustering in the SPC/E simulation is very clearly seen in that the ion−ion component is above 0 for the range 4−14 Å. This is a signature of a stronger ion−ion association in the carbonate solution than in the nitrate solution. This effect is significantly reduced in the POL3 simulation and all but absent in the ECC simulation. The peak at 2.5 Å is due to Ow−ion term and, more specifically, a short strong hydrogen bond present between the Ow and Oi atoms that occurs in the carbonate simulations but not in the nitrate simulations. The peak at 3.2 Å is mostly due to the correlation of the central atom of the oxyanion to Ow and is again associated with the short strong hydrogen bond mentioned above. The peak at 5.8 Å is mostly due to Ow−Ow correlations between water molecules hydrating the oxyanion (Figure S1 in the Supporting Information). Also, in the carbonate solution, the contribution due to the K−O correlation is doubled compared to the nitrate solution due to the former solution having twice the concentration of potassium.

The raw experimental neutron scattering data for the $F(Q)$ functions and the difference $\Delta F(Q)$ are shown in Figure 5.

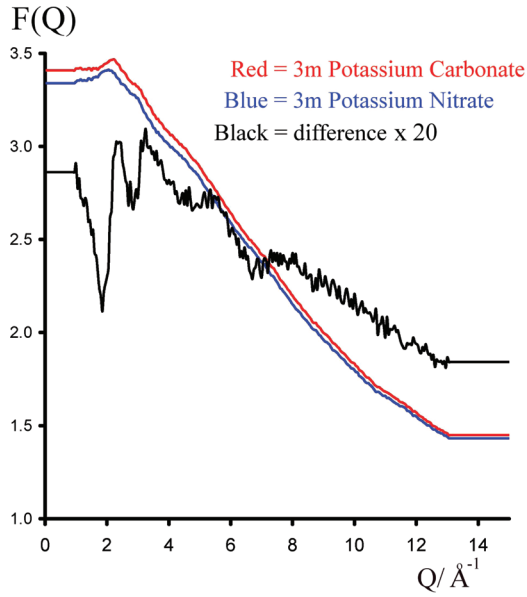

Figure 5. Experimental functions $F(Q)$ (red, K_2CO_3; blue, KNO_3). Also shown on the same scale is the difference function $\Delta F(Q)$ scaled by a factor of 20. The majority of the background curve on the function $F(Q)$ is due to the Placzek effect due to the large amount of ^1H in these samples, which in real space corresponds to a large correlation at unphysically low distances ($r < 1$).

Before both the MD and experimental data can be usefully compared, they must represent identical data ranges. This processing is performed only on the totals $F(Q)$ and $G(r)$. In the current study, there are no correlations of interest that correspond to r-space features at $r < 2.3$ Å. The experimentally measured functions $F(Q)$ from Figure 5 were, therefore, directly transformed to their real space representations and set to the low r limit in the r range 0−2.3 Å prior to being back-transformed to Q space. As can be seen in Figure 6, this has the effect of all but completely removing the Placzek effect (due to inelastic scattering from ^1H) (for method, see ref 29). The Placzek effects in real space constitutes a very strong unphysical feature below 1 Å and the Fourier filtering method is very effective at removing it. For comparability, the MD r-space data ($G(r)$), which are computed directly from the simulations (Figure 4) must also be set to the low r limit in the r range of 0−2.3 Å prior to being back Fourier transformed to the Q-space representation $F(Q)$ (Figure 6). This Q-space data now contain comparable structural data for both the MD and neutron scattering functions. Finally, this data is set to the experimental Q-range (0.9−13 $Å^{-1}$) and transformed to r-space. The data shown in Figure 6 is thus directly comparable between the experiment and MD simu-

dx.doi.org/10.1021/jp3008267 | J. Phys. Chem. B 2012, 116, 8145−8153

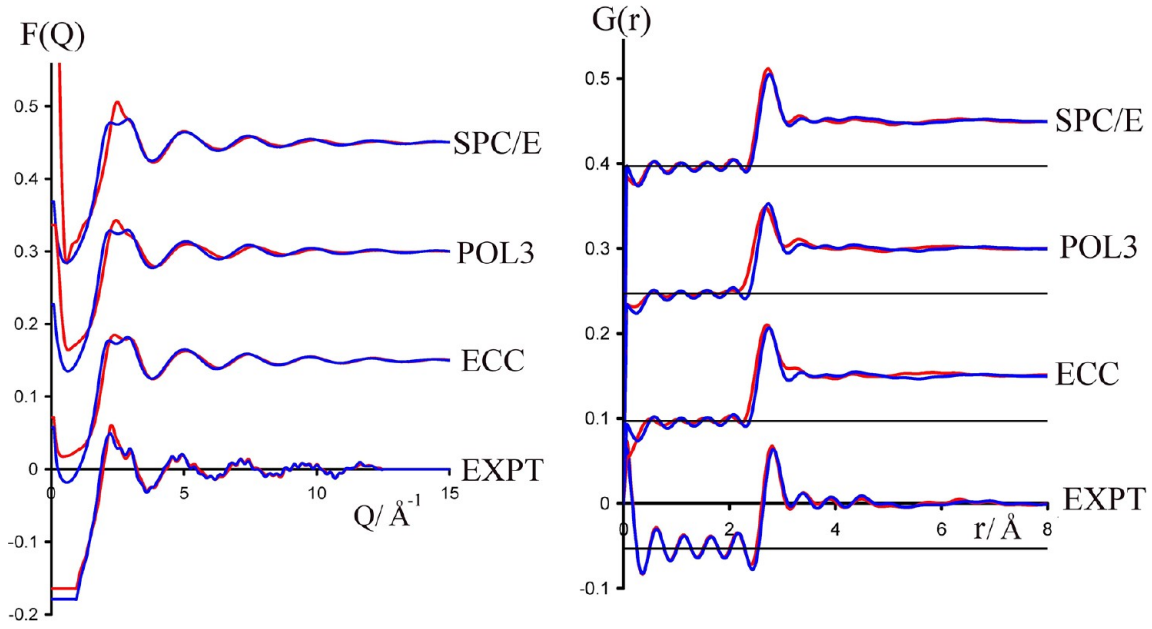

Figure 6. Function $F(Q)$ (left) and its real space representation, the function $G(r)$ (right), with data Fourier-filtered in order to remove all correlations below 2.3 Å. In each case, the carbonate dianion is shown in red, while the nitrate anion is shown in blue. Already at this point, it is clear that the difference between these two functions is better reproduced by the ECC than the SPC/E or POL3 simulations.

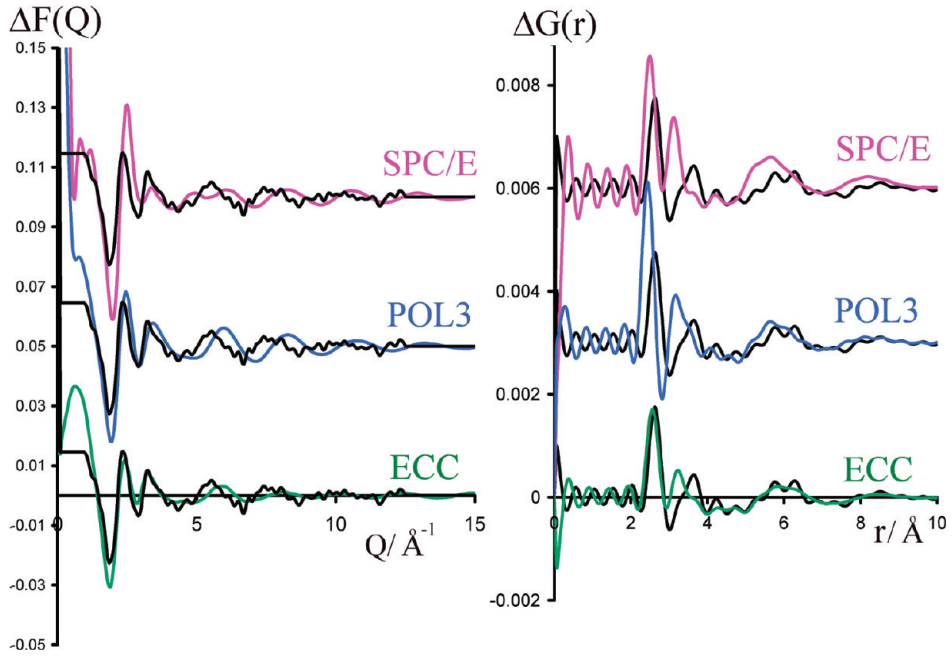

Figure 7. Plots of $\Delta F(Q)$ (left) and $\Delta G(r)$ (right), with the data Fourier-filtered in order to remove all data below 2.3 Å. In each case, the experimental data are shown in black with the data from the SPC/E, POL3, and ECC simulations shown in purple, blue, and green, respectively.

lations; that is, the MD data has now the experimental resolution applied to it. The difference functions $\Delta F(Q)$ and $\Delta G(r)$ are calculated directly from these functions (Figure 7). As has been found previously, the direct comparison of totals between MD and neutron scattering is rather poor (Figure 6), while the comparison of the structural differences between the two solutions ($\Delta F(Q)$ and $\Delta G(r)$, Figure 7) is significantly better.[33] As has been discussed in previous studies,[29] this is due to the large part of the totals relating to $g_{OwOw}(r)$, which is very sensitive to the details of the water model. Thus, it has been found that the $g_{OwOw}(r)$ in various water models (TIP3P, TIP4P, and SPC/E) show a greater variation than might be expected from the resulting three-dimensional water structure.[34] However, in these simulations, the ion−ion/ion−water structure is typically less sensitive to the details of the nonpolarizible water model used (either TIP3P or SPC/E), and this is reflected in the trends (i.e., the difference functions $\Delta F(Q)$and $\Delta G(r)$) being relatively insensitive to water models employed. The same result, i.e., that the difference functions provide better correlations with the experimental data, is also observed in this study (Figure 7). Additionally, the ECC model provides a significantly better fit to the experimental data than either the SPC/E or POL3 models. In particular, it more successfully reproduces the features due to the short strong hydrogen bond of the hydrating water to the

dx.doi.org/10.1021/jp3008267 | J. Phys. Chem. B 2012, 116, 8145−8153

carbonate and the correlations between waters hydrating the carbonate (at ∼6.0 Å; see figure S1, Supporting Information), which are sensitive to the degree of ion clustering as water molecules are displaced by ions in the clusters.

The SPC/E water has a dielectric constant of 68, and by scaling the ionic charges, we have effectively multiplied it by a factor of ∼1.78, yielding a value of 121 instead of the experimental value of 78.[4] To check this effect of overpolarization of water, we performed analogous calculations with the TIP4P water model with ECC charges. The dielectric constant of TIP4P water is 50,[4] yielding 89 for the ECC charges, which is a value closer to the experiment than for SPC/E. Despite this difference, the results of ECC simulations with SPC/E and TIP4P water models are very similar to each other and to the experiment (see Supporting Information).

It may be noted that, prior to performing the ECC simulation, the discrepancy between the SPC/E or POL3 results and the experimental data had bothered us greatly, to the point where we had stalled the completion of this article. Empirically, we tried changing bond lengths, Van der Waals radii of the oxyanion, and changing the ratio of the partial charge on the oxygen and central atom of the oxyanion in the force fields within the SPC/E and POL3 simulations (see Supporting Information), yet significant deviations from experimental data persisted, similar to those found in a comparable study of the high charge density fluoride ion.[33] Indeed, these results were pointing toward fundamental limitations of nonpolarizable molecular dynamics simulations in correctly assessing structure around high charge density species. This result is also concordant with a previous similar study of $Cs_2CO_3/CsNO_3$, which, on close inspection, reveals that nonpolarizible models again overstate the difference between these two solutions compared to the neutron scattering data.[29]

While structural data have been presented to support both strong ion pairing and indeed larger clusters of a form[35,36] not dissimilar to the aggregation found in aqueous solutions of alcohols[37,38] and pyridine,[24,39] it is generally found that ion-pairing in solutions of divalent ions in nonpolarizible water is overstated compared to the experimental data.[13] It should be made clear what is meant by strong ion pairing in this context. For instance, let us take a 1−4 Arg^+−Glu^- salt bridge stabilization in α-helix peptides of about 2−5 kJ/mol[17,40,41] and apply the corresponding binding constant to a 1 M solution of guanidinium acetate (i.e., for the equilibrium ΔG (∼2−5 kJ/mol) = kT ln{[Gdm^+ − Ac^-]/[Gdm^+][Ac^-]} and an initial concentration of GdmAc of 1 M). This assumption means that 50−70% of the ions will be involved in ion pairing. Pragmatically, we use the term strong ion pairing to describe solutes where the level of ion pairing in a denaturant type concentration solution will significantly influence the ability of the counterion to affect the stability of a protein. Traditionally, the Hofmeister ordering of ions[42,43] assumes that the effect the ions have on the stability of the protein does not significantly depend on the counterion. For strongly pairing ions, it is no longer true that the ions act effectively independently and non-Hofmeister behavior is observed. For instance, GdmCl is found to be a strong denaturant of primarily trypophan-stabilized peptide zippers; yet, when the counterion is changed to sulfate, the guanidinium cation loses all its ability to destabilize such peptides.[44] We attribute this to the strong ion pairing, even though the actually binding constants are likely to be in the 2−5 kJ/mol range. Clearly, accurately assessing the level of ion pairing is important in many fields of molecular dynamics.

CONCLUSIONS

By comparing molecular dynamics simulations and neutron scattering data, the present study presents an efficient and accurate way for modeling aqueous solutions of multivalent ions, focusing on the environmentally important carbonate dianion. Simulations in SPC/E and POL3 water both predict the formation of extended (nanometer-size) and persistent ion clusters in the K_2CO_3 solution, while this largely artificial feature is hardly present in the ECC simulation. When $\Delta F(Q)$ or $\Delta G(r)$ functions from the simulations are compared to neutron scattering structural data, the SPC/E simulation provides a rather poor comparison, while the ECC (but not POL3) simulation shows a significantly better agreement. The simplistic empirical observation of the height of the potassium−oxyanion peak in the radial distribution function (Figure 2) suggests that ion-pairing in POL3, with about 50% of the polarizibility of real water, is about halfway from SPC/E (with no polarizibility) to the ECC simulations (effectively accounting for 100% of polarizibility). This indicates that polarizibility is indeed a significant effect and needs to be taken into account in aqueous electrolyte simulations, particularly if multivalent ions are present. Future work on different systems will show what is the general applicability and accuracy of the simple and promising ECC approach. At the same time, we will learn better what are the limitations of the assumption of the continuum character of the electronic dielectric response of the solvent, which is inherent to this model.

ASSOCIATED CONTENT

Supporting Information

A figure displaying the hydration of the carbonate ion and results from additional empirical fitting of a nonpolarizible carbonate force field. This material is available free of charge via the Internet at http://pubs.acs.org.

AUTHOR INFORMATION

Corresponding Author

*E-mail: philip.mason@uochb.cas.cz (P.E.M.); pavel.jungwirth@uochb.cas.cz (P.J.).

Notes

The authors declare no competing financial interest.

A video summary of this work can be found at http://www.youtube.com/watch?v=q5NzDecddxY.

ACKNOWLEDGMENTS

Support from the Czech Science Foundation (grant 203/08/0114) is gratefully acknowledged. P.J. thanks the Academy of Sciences for the Praemium Academie award. P.E.M. thanks Gabriel Cuello and the D20 staff of the Institut Laue Langevin for their help with the neutron scattering experiments.

REFERENCES

(1) Takahashi, T.; Sutherland, S. C.; Sweeney, C.; Poisson, A.; Metzl, N.; Tilbrook, B.; Bates, N.; Wanninkhof, R.; Feely, R. A.; Sabine, C.; Olafsson, J.; Nojiri, Y. *Deep-Sea Res., Part II* **2002**, *49* (9−10), 1601−1622.

(2) Orr, J. C.; Fabry, V. J.; Aumont, O.; Bopp, L.; Doney, S. C.; Feely, R. A.; Gnanadesikan, A.; Gruber, N.; Ishida, A.; Joos, F.; et al. *Nature* **2005**, *437* (7059), 681−686.

(3) Mark, P.; Nilsson, L. *J. Phys. Chem. A* **2001**, *105* (43), 9954−9960.

(4) Vega, C.; Abascal, J. L. F. *Phys. Chem. Chem. Phys.* **2011**, *13* (44), 19663−19688.

(5) Leontyev, I.; Stuchebrukhov, A. *Phys. Chem. Chem. Phys.* **2011**, *13* (7), 2613−2626.
(6) Leontyev, I. V.; Stuchebrukhov, A. A. *J. Chem. Phys.* **2009**, *130*, 8.
(7) Leontyev, I. V.; Stuchebrukhov, A. A. *J. Chem. Theory Comput.* **2010**, *6* (5), 1498−1508.
(8) Leontyev, I. V.; Stuchebrukhov, A. A. *J. Chem. Theory Comput.* **2010**, *6* (10), 3153−3161.
(9) Rahman, A.; Stillinger, F. *J. Chem. Phys.* **1971**, *55* (7), 3336.
(10) Leontyev, I. V.; Vener, M. V.; Rostov, I. V.; Basilevsky, M. V.; Newton, M. D. *J. Chem. Phys.* **2003**, *119* (15), 8024−8037.
(11) Guvench, O.; Mallajosyula, S. S.; Raman, E. P.; Hatcher, E.; Vanommeslaeghe, K.; Foster, T. J.; Jamison, F. W.; MacKerell, A. D. *J. Chem. Theory Comput.* **2011**, *7* (10), 3162−3180.
(12) MacKerell, A. D.; Bashford, D.; Bellott, M.; Dunbrack, R. L.; Evanseck, J. D.; Field, M. J.; Fischer, S.; Gao, J.; Guo, H.; Ha, S.; et al. *J. Phys. Chem. B* **1998**, *102* (18), 3586−3616.
(13) Wernersson, E.; Jungwirth, P. *J. Chem. Theory Comput.* **2010**, *6* (10), 3233−3240.
(14) Lamoureux, G.; Roux, B. *J. Phys. Chem. B* **2006**, *110* (7), 3308−3322.
(15) Soper, A. K.; Weckstrom, K. *Biophys. Chem.* **2006**, *124* (3), 180−191.
(16) Mason, P. E.; Neilson, G. W.; Dempsey, C. E.; Barnes, A. C.; Cruickshank, J. M. *Proc. Natl. Acad. Sci. U.S.A.* **2003**, *100* (8), 4557−4561.
(17) Dzubiella, J. *J. Am. Chem. Soc.* **2008**, *130* (42), 14000−14007.
(18) Mason, P. E.; Dempsey, C. E.; Vrbka, L.; Heyda, J.; Brady, J. W.; Jungwirth, P. *J. Phys. Chem. B* **2009**, *113* (10), 3227−3234.
(19) Ratheal, I. M.; Virgin, G. K.; Yu, H. B.; Roux, B.; Gatto, C.; Artigas, P. *Proc. Natl. Acad. Sci. U.S.A.* **2010**, *107* (43), 18718−18723.
(20) Schneider, C. P.; Shukla, D.; Trout, B. L. *J. Phys. Chem. B* **2011**, *115* (22), 7447−7458.
(21) McLain, S. E.; Soper, A. K.; Daidone, I.; Smith, J. C.; Watts, A. *Angew. Chem., Int. Ed.* **2008**, *47* (47), 9059−9062.
(22) Hansen, T. C.; Henry, P. F.; Fischer, H. E.; Torregrossa, J.; Convert, P. *Meas. Sci. Technol.* **2008**, *19* (3), 034001.
(23) Mason, P. E.; Neilson, G. W.; Barnes, A. C.; Enderby, J. E.; Brady, J. W.; Saboungi, M. L. *J. Chem. Phys.* **2003**, *119* (6), 3347−3353.
(24) Mason, P. E.; Neilson, G. W.; Dempsey, C. E.; Price, D. L.; Saboungi, M. L.; Brady, J. W. *J. Phys. Chem. B* **2010**, *114* (16), 5412−5419.
(25) Caldwell, J. W.; Kollman, P. A. *J. Phys. Chem.* **1995**, *99* (16), 6208−6219.
(26) Berendsen, H. J. C.; Grigera, J. R.; Straatsma, T. P. *J. Phys. Chem.* **1987**, *91* (24), 6269−6271.
(27) Case, D. A.; Darden, T. A.; Cheatham, T. E., III; Simmerling, C. L.; Wang, J.; Duke, R. E.; Luo, R.; Crowley, M. R. C. W.; Zhang, W.; Merz, K. M.; et al. *Amber 10*; University of California: San Francisco, CA, 2008.
(28) Chang, T. M.; Dang, L. X. *J. Phys. Chem. B* **1999**, *103* (22), 4714−4720.
(29) Mason, P. E.; Neilson, G. W.; Dempsey, C. E.; Brady, J. W. *J. Am. Chem. Soc.* **2006**, *128* (47), 15136−15144.
(30) Sass, R. L.; Vidale, R.; Donohue, J. *Acta Crystallogr.* **1957**, *10* (9), 567−570.
(31) Thole, B. T. *Chem. Phys.* **1981**, *59* (3), 341−350.
(32) Berendsen, H. J. C.; Postma, J. P. M.; Vangunsteren, W. F.; Dinola, A.; Haak, J. R. *J. Chem. Phys.* **1984**, *81* (8), 3684−3690.
(33) Mason, P. E.; Heyda, J.; Fischer, H. E.; Jungwirth, P. *J. Phys. Chem. B* **2010**, *114* (43), 13853−13860.
(34) Mason, P. E.; Brady, J. W. *J. Phys. Chem. B* **2007**, *111* (20), 5669−5679.
(35) Mason, P. E.; Dempsey, C. E.; Neilson, G. W.; Brady, J. W. *J. Phys. Chem. B* **2005**, *109* (50), 24185−24196.
(36) Mason, P. E.; Neilson, G. W.; Kline, S. R.; Dempsey, C. E.; Brady, J. W. *J. Phys. Chem. B* **2006**, *110* (27), 13477−13483.
(37) Dixit, S.; Soper, A. K.; Finney, J. L.; Crain, J. *Europhys. Lett.* **2002**, *59* (3), 377−383.
(38) Bowron, D. T.; Finney, J. L.; Soper, A. K. *J. Phys. Chem. B* **1998**, *102* (18), 3551−3563.
(39) Bako, I.; Palinkas, G.; Dore, J. C.; Fischer, H.; Jovari, P. *Chem. Phys. Lett.* **2004**, *388* (4−6), 468−472.
(40) Olson, C. A.; Spek, E. J.; Shi, Z. S.; Vologodskii, A.; Kallenbach, N. R. *Proteins: Struct., Funct., Genet.* **2001**, *44* (2), 123−132.
(41) Scholtz, J. M.; Qian, H.; Robbins, V. H.; Baldwin, R. L. *Biochemistry* **1993**, *32* (37), 9668−9676.
(42) Hofmeister, F. *Arch. Exp. Pathol. Pharmakol.* **1888**, *24*, 247−260.
(43) Kunz, W.; Henle, J.; Ninham, B. W. *Curr. Opin. Colloid Interface Sci.* **2004**, *9* (1−2), 19−37.
(44) Dempsey, C. E.; Mason, P. E.; Bracly, J. W.; Neilson, G. W. *J. Am. Chem. Soc.* **2007**, *129* (51), 15895−15902.
(45) Humphrey, W.; Dalke, A.; Schulten, K. *J. Mol. Graph.* **1996**, *14* (1), 33-8, 27-8.